Cu-X-bpy (X = Cl, Br; bpy = 4,4′-bipyridine) Coordination Polymers: The Stoichiometric Control and Structural Relations of $^{2}_{\infty}[Cu_2X_2(bpy)]$ and $^{3}_{\infty}[CuBr(bpy)]$

Jack Y. Lu, Brenda R. Cabrera, Ru-Ji Wang, and Jing Li*

Department of Chemistry, Rutgers University, Camden, New Jersey 08102

Received May 17, 1999

Introduction

Enormous efforts have recently been made in synthesizing new coordination polymers of 1D, 2D, and 3D structures.[1,2] Incorporation of both organic and inorganic components in these compounds has created a new dimension in searching for functional materials that have desired structures and properties. While a majority of synthetic procedures still follow conventional solution routes, increasing interests have been paid to the less conventional solvothermal technique.[3−5] Our recent studies on the transition-metal bipyridine systems[6−9] have shown that hydrothermal reactions are often sensitive to certain experimental parameters, such as temperature, solvent, stoichiometry, and pH level. Here we report the synthesis and crystal structures of three Cu-X-bpy (X = Cl, Br) compounds, the two-dimensional $^{2}_{\infty}[Cu_2X_2(bpy)]$ and three-dimensional $^{3}_{\infty}[CuBr(bpy)]$, and illustrate how stoichiometry plays a vital role in affecting the product formation, their structures and topology.

Experimental Section

Chemicals and Reagents. All chemicals were used as purchased without further purification, including $CuCl_2 \cdot 2H_2O$ (99+%, Aldrich), $CuBr_2$ (99%, Cerac), and 4,4′-bypyridine (98%, Alfa Aesar).

Synthesis of $^{2}_{\infty}[Cu_2Cl_2(bpy)]$ (I). Orange crystals of **I** were grown from hydrothermal reactions of $CuCl_2 \cdot 2H_2O$ (0.1705 g), bpy (0.1562 g), and H_2O (8 mL) in the mole ratio of 1:1:444 in a 23 mL acid digestion bomb at 170 °C for 7 days. The product was washed with water and acetone and dried in air. **I** was isolated as a single-phase product.

Synthesis of $^{2}_{\infty}[Cu_2Br_2(bpy)]$ (II). Reactions of $CuBr_2$ (0.2234 g), bpy (0.1562 g) and H_2O (3 mL) in the mole ratio of 1:1:167 in a 23 mL acid digestion bomb resulted in dark yellow crystals of **II**. The same experimental conditions as described for **I** were applied to these reactions.

Synthesis of $^{3}_{\infty}[CuBr\ (bpy)]$ (III). Crystal growth of **III** was carried out under identical reaction conditions as for both **I** and **II**, except that the amount of the bpy used was doubled ($CuBr_2$ (0.2234 g), bpy (0.3124 g), and H_2O (3 mL) in the mole ratio of 1:2:167). The product contained dark red crystals of **III** in quantitative yield.

Crystallographic Studies. An orange crystal of **I** (0.03 × 0.2 × 0.32 mm), a dark yellow crystal of **II** (0.05 × 0.1 × 0.5 mm), and a dark red crystal of **III** (0.2 × 0.2 × 0.5 mm) were selected for the structure analysis. The intensity data of **I** were collected on an Rigaku R-AXIS IIc area at 296 K. Indexing was performed from a series of 1° oscillation images with exposures of 8 min per frame. A hemisphere of data was collected using 12° oscillation angles with exposures of 5 min per frame and a crystal-to-detector distance of 82 mm. Oscillation images were processed using bioteX,[10] producing a listing of unaveraged F^2 and $\sigma(F^2)$ values which were then passed to the teXsan[11] program package for further processing and structure solution on a Silicon Graphics Indigo R4000 computer. A total of 4499 reflections were measured over the ranges $6.4 \le 2\theta \le 50.68°$, $-4 \le h \le 4$, $-15 \le k \le 15$, $-13 \le l \le 13$, yielding 1000 unique reflections. The intensity data were corrected for Lorentz and polarization effects and for absorption using REQAB[12] and the structure was solved by direct methods (SIR92[13]). Non-hydrogen atoms were refined anisotropically and hydrogen atoms were refined using a "riding" model. Data collection of **II** and **III** were carried out on an Enraf-Nonius CAD4 automated diffractometer at 295 K. Twenty-five reflections were centered in each case using graphite-monochromated Mo Kα radiation. All data were collected with ω scan method within the limits $6 \le 2\theta \le 50°$. Raw data were corrected for Lorentz and polarization effects, and an empirical absorption correction was applied in each case. The structures were solved using the SHELX-97 program.[14] Non-hydrogen atoms were located by direct phase determination and subjected to anisotropic refinement. The full-matrix least-squares calculations on F^2 were applied on the final refinements. The unit cell parameters, along with data collection and refinement details, are tabulated in Table 1. Final atomic coordinates and average temperature factors are listed in Tables 2−4. Crystal drawings were generated by SCHAKAL 92.[15]

X-ray powder diffraction analyses were performed on a Rigaku D/M-2200T automated diffraction system (Ultima$^+$). All measurements were made between a 2θ range of 5 and 80° at the operating power of 40 kV/40 mA.

Thermal Analysis. Thermogravimetric (TGA) analyses of the title compounds were performed on a computer controlled TA Instrument 2050TGA analyzer. Single-phase powder samples of **I** (20.973 mg), **II** (35.322 mg), and **III** (18.476 mg) were loaded into alumina pans and heated with a ramp rate of 1 °C/min from room temperature to 850 °C.

* To whom correspondence should be addressed.

(1) Robson, R. In *Comprehensive Supramolecular Chemistry*; Pergamon: New York, 1996: Chapter 22, pp 733−755. Batten, S. R.; Robson, R. *Angew. Chem., Int. Ed.* **1998**, *37*, 1460.
(2) Zaworotko, M.; Rogers, R. D. In *Synthesis of New Materials by Coordination Chemistry Self-Assembly and Template Formation*; **1999**.
(3) Gutschke, S. O. H.; Slawin, A. M. Z.; Wood, P. T. *J. Chem. Soc., Chem. Commun.* **1995**, 2197. Gutschke, S. O. H.; Molinier, M.; Powell, A. K.; Winpenny, E. P.; Wood, P. T. *Chem. Commun.* **1996**, 823.
(4) Yaghi, O. M.; Li, H. *J. Am. Chem. Soc.* **1996**, *118*, 295. Yaghi, O. M.; Li, H. *J. Am. Chem. Soc.* **1996**, *118*, 10401. Reineke, T. M.; Eddaoudi, M.; Fehr, M.; Kelley, D.; Yaghi, O. M. *J. Am. Chem. Soc.* **1999**, *121*, 1651.
(5) Hagrman, D.; Hammond, R. P.; Haushalter, R.; Zubieta, J. *Chem. Mater.* **1998**, *10*, 2091. Hammond, R. P.; Cavaluzzi, M.; Haushalter, R. C.; Zubiata, J. A. *Inorg. Chem.* **1999**, *38*, 1288.
(6) Lu, J. Y.; Cabrera, B. R.; Wang, R.-J.; Li, J. *Inorg. Chem.* **1998**, *37*, 4480.
(7) Lu, J. Y.; Lawandy, M. A.; Li, J. Yuen, T.; Lin, C. L. *Inorg. Chem.* **1999**, *38*, 2695.
(8) Cabrera, B. R.; Wang, R.-J.; Li, J.; Yuen, T. in *Solid State Chemistry of Inorganic Materials II*, Proceedings of the Symposium of the Materials Research Society, Boston, MA, November 30−December 4, 1998; Materials Research Society: Warrendale, PA, 1999; pp 493−498.
(9) Lawandy, M. A.; Huang, X.-Y.; Lu, J. Y.; Li, J.; Yuen, T.; Lin, C. L. *Inorg. Chem.*, accepted.
(10) *Biotex: A suite of Programs for the Collection, Reduction and Interpretation of Imaging Plate Data*; Molecular Structure Corporation: The Woodlands, TX, 1995.
(11) *teXsan: Crystal Structure Analysis Package*; Molecular Structure Corporation: The Woodlands, TX, 1985 & 1992.
(12) *REQAB*; private communication, R. Jacobsen, 1994.
(13) *SIR92*; Altomare, A.; Burla, M. C.; Camalli, M.; Cascarano, M.; Giacovazzo, C.; Guagliardi, A.; Polidoro, G. 1994. *J. Appl. Crystallogr.*, **27**, 435.
(14) Sheldrick, G. M. *SHELX-97: Program for structure refinement*; University of Göttingen: Germany, 1997.
(15) Keller, E. *SCHAKAL 92: A computer program for the graphical representation of crystallographic models*; University of Freiburg: Germany, 1992.

10.1021/ic990536p CCC: $18.00
Published on Web 09/16/1999

Table 1. Crystallographic Data for **I**, **II**, and **III**

	I	**II**	**III**
formula	$Cu_2C_{10}H_8N_2Cl_2$	$Cu_2C_{10}H_8N_2Br_2$	$CuC_{10}H_8N_2Br$
fw	345.16	443.08	299.63
space group	$P2_1/c$ (No. 14)	$P2_1/c$ (No. 14)	$I4_1/acd$ (No.)
a, Å	3.7961(1)	3.909(1)	14.406(2)
b, Å	12.7478(1)	12.752(3)	
c, Å	11.5244(5)	11.905(2)	38.524(8)
β, deg	94.910(4)	94.05(3)	
V, Å^3	555.64(4)	592.0(2)	7995(2)
Z	2	2	32
ρ_{calcd}, g cm^{-3}	2.117	2.486	1.991
μ, mm^{-1}	4.274	10.311	6.140
R [$I > 4\sigma(I)$] R1	0.0469	0.0297	0.0303
wR2	0.1155	0.0481	0.0520

[a] $R1 = \sum||F_o| - |F_c||/\sum|F_o|$. , [b] $wR2 = \sqrt{\sum[w(F_o^2-F_c^2)^2]/\sum w(F_o^2)^2}$, $w = 1/[\sigma^2(F_o^2) + 55.02P]$, $P = (F_o^2 + 2F_c^2)/3$ for **I**, $w = 1/[\sigma^2(F_o^2) + (0.0202P)^2 + 0.91P]$, $P = (F_o^2 + 2F_c^2)/3$ for **II**, $w = 1/[\sigma^2(F_o^2) + 0.0498P^2 + 1.3878P]$, $P = (F_o^2 + 2F_c^2)/3$ for **III**.

Table 2. Positional Parameters and *U*(eq)[a] for **I**

atom	*x*	*y*	*z*	U_{eq}
Cu	0.2371(2)	0.07385(6)	0.94662(7)	0.0615(3)
Cl	0.6912(3)	0.00137(10)	0.85298(10)	0.0426(4)
N1	0.1502(11)	0.2265(3)	0.9675(4)	0.0413(10)
C2	0.2542(14)	0.2773(4)	1.0668(4)	0.0468(13)
H2	0.3688(14)	0.2394(4)	1.1277(4)	0.07(2)
C3	0.1991(14)	0.3829(4)	1.0826(4)	0.0447(12)
H3	0.2755(14)	0.4143(4)	1.1531(4)	0.05(2)
C4	0.0292(12)	0.4429(4)	0.9934(4)	0.0344(10)
C5	−0.0763(14)	0.3895(4)	0.8913(4)	0.0412(11)
H5	−0.1892(14)	0.4255(4)	0.8285(4)	0.05(2)
C6	−0.0149(14)	0.2840(4)	0.8828(4)	0.0463(12)
H6	−0.0931(14)	0.2504(4)	0.8137(4)	0.05(2)

[a] *U*(eq) is defined as one third of the trace of the orthogonalized $\mathbf{U}_{ij}$ tensor.

Table 3. Positional Parameters and *U*(eq)[a] for **II**

atom	*x*	*y*	*z*	*U*(eq)
Br(1)	0.19469(12)	0.50444(4)	0.34746(4)	0.03784(16)
Cu(1)	0.26651(19)	0.42729(5)	0.54390(5)	0.0523(2)
N(1)	0.3426(10)	0.2726(3)	0.5272(3)	0.0369(10)
C(1)	0.4678(12)	0.0574(3)	0.5057(4)	0.0299(10)
C(2)	0.5044(13)	0.2168(4)	0.6104(4)	0.0419(13)
C(3)	0.5691(12)	0.1117(4)	0.6027(4)	0.0368(13)
C(4)	0.3022(13)	0.1157(4)	0.4198(4)	0.0437(14)
C(5)	0.2494(13)	0.2205(4)	0.4341(4)	0.0434(13)

[a] *U*(eq) is defined as one-third of the trace of the orthogonalized $\mathbf{U}_{ij}$ tensor.

Results and Discussion

Recent studies by us and by others have shown the tendency of Cu(I) to form one-dimensional ribbonlike structural moiety with helogens (X = Cl, Br) under hydrothermal conditions.[5−6,8] The Cu_2X_2 ribbons are formed by connecting the two CuX zigzag single chains via Cu−X bonds, as shown in Scheme 1. The copper atoms in the resultant ribbon structure have a 3-fold coordination with X atoms, leaving one site available for the fourth bond with an additional ligand. The bidentate 4,4′-bipyridine is one of the most reactive rodlike rigid ligands and is therefore a good choice for the fourth coordination of Cu in the Cu_2X_2 double-chain. The construction of a two-dimensional layered network by connecting the ribbons through the bridging bpy via copper−nitrogen bonds should therefore not be too difficult to visualize (see Scheme 2).

The actual crystal structure of **I** and **II** consists of the aforementioned Cu_2X_2(bpy) (X = Cl, Br) two-dimensional

Table 4. Positional Parameters and *U*(eq)[a] for **III**

atom	*x*	*y*	*z*	*U*(eq)
Br(1)	0.60405(3)	0.34706(3)	0.031306(13)	0.04675(17)
Cu(2)	0.43207(4)	0.32059(4)	0.017750(14)	0.04506(19)
N(1)	0.4111(2)	0.3376(2)	−0.03243(8)	0.0351(8)
N(2)	0.3738(2)	0.3939(3)	0.05607(9)	0.0375(9)
C(1)	0.4062(3)	0.3432(3)	−0.10579(9)	0.0296(9)
C(2)	0.32175(16)	0.46939(17)	0.05022(6)	0.0394(12)
C(3)	0.28982(16)	0.49164(17)	0.11072(6)	0.0281(10)
C(4)	0.34574(16)	0.41434(17)	0.11668(6)	0.0357(11)
C(5)	0.2798(3)	0.5182(3)	0.07684(10	0.0355(11)
C(6)	0.3846(3)	0.3693(3)	0.08936(10)	0.0402(11)
C(7)	0.4550(3)	0.4029(3)	−0.05114(13)	0.0421(12)
C(8)	0.3585(4)	0.2771(3)	−0.08707(13)	0.0465(13)
C(9)	0.4544(3)	0.4083(3)	−0.08637(12)	0.0398(12)
C(10)	0.3627(4)	0.2772(3)	−0.05155(13)	0.0500(14)

[a] *U*(eq) is defined as one-third of the trace of the orthogonalized $\mathbf{U}_{ij}$ tensor.

Scheme 1

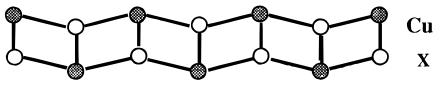

Scheme 2

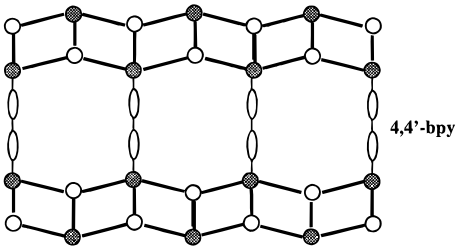

network stacking along the crystallographic *b* axis. Two views along the *c* and *a* axes are shown in Figure 1. All Cu(I) atoms in the Cu_2X_2 double-chain are 3-fold coordinated to X, and all X atoms also bridge to three copper metal centers giving Cu−X distances varying from 2.304(1) to 2.494(1) Å (**I**) and from 2.452(1) to 2.546(1) Å (**II**). These are comparable with those reported for [CuCl(bpy)],[16] $[(CuCl)_2(C_{10}H_7N_3)]$,[6] $[(C_{10}H_8N_2)_2(CuBr)]Cu_3Br_4$,[8] and $[(CuBr)_3(C_{10}H_7N_3)]$.[6] Each 4,4′-bpy binds to two different copper atoms via its N sites which completes the fourth coordination of Cu(I) with a stable and preferred tetrahedral geometry. The Cu−N distances (**I**, 1.991(4) Å; **II**, 2.007(4) Å) also compare well with those found in $[(C_{10}H_8N_2)_2(CuBr)]Cu_3Br_4$ and in $[(CuBr)_3(C_{10}H_7N_3)]$. There is also a weak Cu−Cu interaction in the double-chain characterized by a distance of 2.927(1) Å.

The synthesis described in the previous section shows that the formation of **II** and **III** is largely controlled by the reaction stoichiometry. While mixing of copper bromide with bpy in a 1:1 ratio yielded **II** as the reaction product, increasing bpy by a factor of 2 (1:2 ratio) produced **III** in quantitative yield. The chlorine analogue of **III** can also be obtained in quantitative yield under the similar conditions. The structure of **III** is a three-dimensional network consisting of four interlocking planar lattices.[16] Some structural relations may be drawn between these planar lattices and the 2D structures of **I** and **II**. This is illustrated in Scheme 3. By replacing every other pair of Cu−X bond in the Cu_2X_2 double-chains (ribbons) with two Cu−N bonds made through the additional 4,4′-bpy (each dotted line signifying a 4,4′-bpy added to the original structure), one would

(16) Yaghi, O. M.; Li, G. *Angew. Chem., Int. Ed. Engl.* **1995**, *34*, 207.

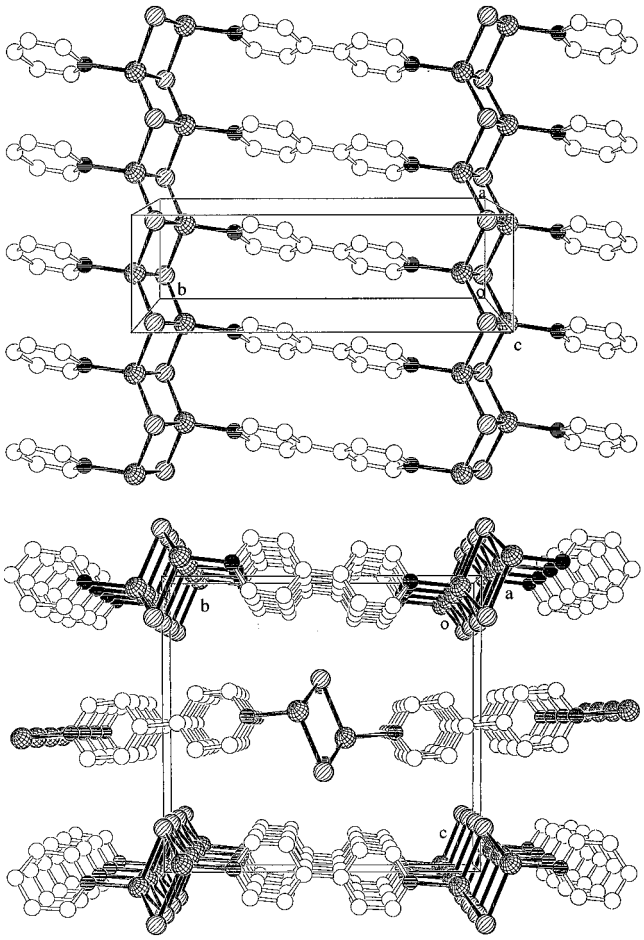

Figure 1. Two perspective views of the two-dimensional structure of $^{2}_{\infty}$[(CuX)$_2$bpy] (**I** and **II**) (X = Cl, Br) along the *c* (top) and *a* (bottom) axes. The cross-shaded circles are Cu atoms, the solid circles are N atoms, the shaded circles are X atoms, and the open circles are C atoms, respectively. The H atoms are omitted for clarity.

Scheme 3

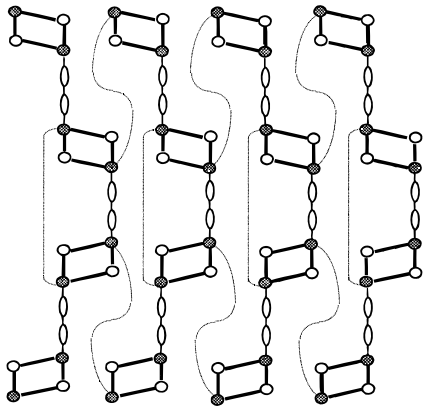

$Cu_2X_2(bpy) + bpy$

arrive at a two-dimensional network as shown in Scheme 4. The stoichiometry of this motif is now $Cu_2X_2(bpy)_2$, or simply CuX(bpy), and its actual crystal structure is shown in Figure 2. Four of these nets interlock to give rise to a three-dimensional network structure, as depicted in Figure 3a. No bonds are involved among the interlocking two-dimensional nets. The four crystallographically identical yet topologically independent planar networks can be grouped into two sets, one with two vertical and parallel nets and the other with two horizontal and

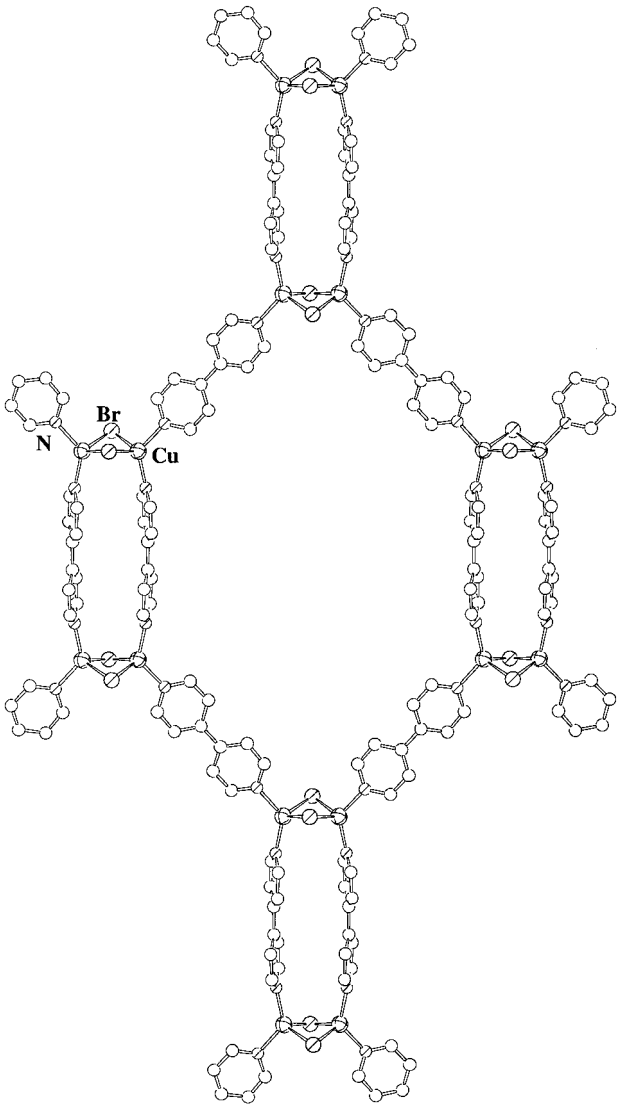

Figure 2. Structure of the interlocking planar net in $^{3}_{\infty}$[CuBr(bpy)] (**III**). The octagonal ring is shown in the center. The cross-shaded circles are Cu atoms, the singly shaded circles are Br atoms (large) and N atoms (small), and the open circles are C atoms.

Scheme 4

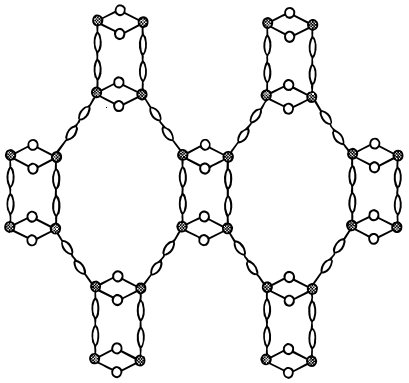

$Cu_2X_2(bpy)_2 \equiv CuX\,(bpy)$

parallel nets. They are concatenated through mutual interpenetration at 90° to give a three-dimensional framework structure (see Figure 3b).

Each interpenetrating planar net is composed of large octagonal rings, each formed by sharing four 4,4′-bipyridines

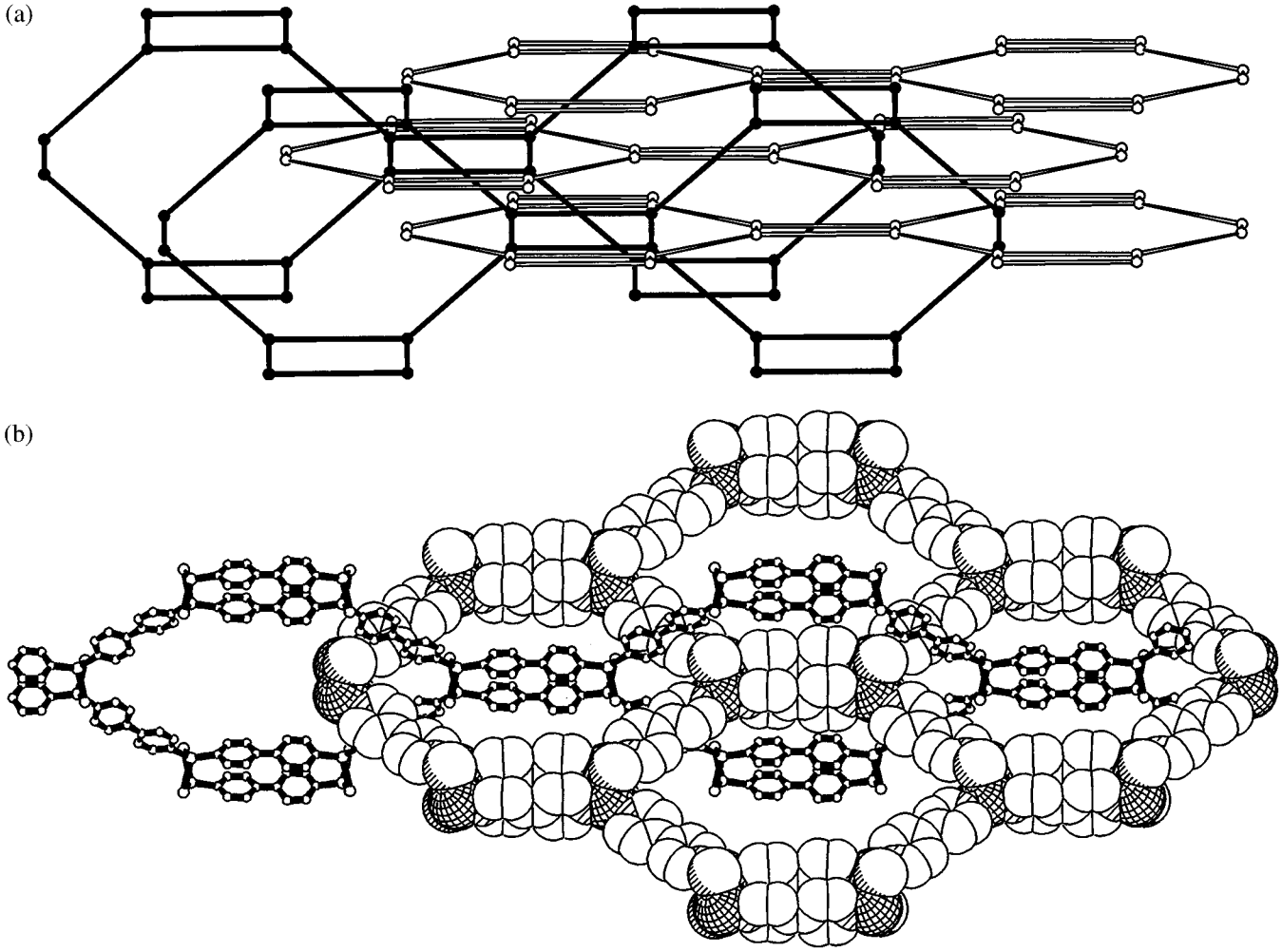

Figure 3. (a) Four independent interlocking planar nets in **III**. The copper atoms are represented by open and solid circles, and bpy ligands by open and solid lines. The Br atoms are omitted for clarity. Note that the third horizontal net is generated by the first by an $\boldsymbol{a} + \boldsymbol{b}$ translation. (b) Two perpendicular interlocking nets shown concatenated at 90°. The space-filling model represents the horizontal net and the ball-and-stick model for the vertical net. Other two are omitted for clarity.

and four $[(Cu_2Br_2)(4,4'\text{-bpy})]_2$ rectangular units with eight adjacent octagonal rings. The approximate dimensions of these octagonal rings are 28 Å × 18 Å (Figure 2). The two pyridine rings in the two independent bpy are twisted by 18.1° and 19.9°, respectively. As shown in Figure 3a, each octagonal unit is interlocked with a pair of perpendicular and rectangle-linked octagonal rings and two pairs of bpy edge-sharing octagonal rings above and below the former. The interpenetration seems necessary to stabilize the structure with empty space inside the large cages. Copper atoms are in distorted tetrahedral sites with its bond angles ranging from 100.2(1) to 126.4(1)°. They compare well with those found in its chloride analogue (99.6(4)−125.6(6)°).[16] The Cu−Cu distance is 2.823(1) Å, slightly longer than that found in CuCl(bpy). The Cu−N distances vary from 1.972(3) to 2.000(3) Å, comparable with those found in **II** (2.007(4) Å) and $[(CuBr)_3(C_{10}H_7N_3)]$ (2.004(2) Å).[6] Each bromine atom forms a bridge between two tetrahedral Cu atoms. The Cu−Br distances range from 2.525(1) to 2.561(1) Å, also comparable to those in **II** and in $[(CuBr)_3(C_{10}H_7N_3)]$.

Thermal analyses were performed on a TA 2050TGA instrument. The results measured from room temperature to 850 °C indicated that both **I** and **II** are thermally stable up to 250 °C whereas **III** starts to decompose around 220 °C. The residues of **I** were identified to be copper metal by X-ray powder diffraction taken immediately after the TGA experiment.

Acknowledgment. Financial support from the National Science Foundation (DMR-9553066 and REU Supplement funds) is greatly appreciated. The FT-IR/TGA/DSC apparatus was purchased through a NSF ARI grant (CHE 9601710-ARI).

Supporting Information Available: Tables of crystal structural data, atomic coordinates, anisotropic and isotropic parameters of all non-hydrogen atoms, structural factors and three ORTEP drawings with 50% thermal vibrational ellipsoids. This material is available free of charge via the Internet at http://pubs.acs.org.

IC990536P